

Lattice QCD study of the $I = 0$ scalar channel using four-quark operators

SCALAR Collaboration: Teiji Kunihiro^a, Shin Muroya^b, Atsushi Nakamura^{c,d,e,f}, Chiho Nonaka^{g,h}, Motoo Sekiguchiⁱ, Hiroaki Wada^j and Masayuki Wakayama^{*†g}

^a*Department of Physics, Kyoto University, Kyoto 606-8502, Japan*

^b*Department of Comprehensive Management, Matsumoto University, Matsumoto 390-1295, Japan*

^c*Research Institute for Information Science and Education (RIISE), Hiroshima University, Higashi-Hiroshima 739-8521, Japan*

^d*Research Center for Nuclear Physics (RCNP), Osaka University, Ibaraki 567-0047, Japan*

^e*Theoretical Research Division, Nishina Center, RIKEN, Wako 351-0198, Japan*

^f*School of Biomedicine, Far Eastern Federal University, Vladivostok 690950, Russia*

^g*Department of Physics, Nagoya University, Nagoya 464-8602, Japan*

^h*Kobayashi Maskawa Institute (KMI), Nagoya University, Nagoya 464-8602, Japan*

ⁱ*School of Science and Engineering, Kokushikan University, Tokyo 154-8515, Japan*

^j*Faculty of Political Science and Economics, Kokushikan University, Tokyo 154-8515, Japan*

We investigate the possible significance of four-quark states in the $I=0$ scalar channel by performing two-flavor full lattice QCD simulations on an $8^3 \times 16$ lattice using the improved gauge action and the clover-improved Wilson quark action.

The 33rd International Symposium on Lattice Field Theory

14 -18 July 2015

*Kobe International Conference Center, Kobe, Japan**

*Speaker.

†E-mail: wakayama@hken.phys.nagoya-u.ac.jp (M. Wakayama)

1. Introduction

The nature of the light nonet scalar mesons continues to be an interesting problem in hadron physics. The sigma resonance in $I=J=0$ channel is now accepted since pole was determined in precise and systematic analyses of the π - π scattering respecting the crossing symmetry as well as the chiral symmetry. The Particle Data Group (PDG) summary quotes a mass of the σ in the range 400 to 700 MeV[1]. The significance of the σ meson is closely related to the chiral symmetry in QCD. The σ meson may be identified a chiral partner of the π in the linear representations of $SU(2) \times SU(2)$ symmetry. However, the physical content and the mechanism for realizing such a light state in the $J^{PC}=0^{++}$ state is still not well understood. Most popular ideas is the tetraquark proposed by Jaffe[2], who showed that the color magnetic interaction between the di-quark and anti-di-quark gives a large attraction to down the masses of the scalar mesons around 600 MeV. On the other hand, most simple idea is that the wave function of the σ meson also have components of the molecule states. Recently, these have been many new states that have been discovered such as the $X(3872)$, $Y(4260)$, $Z(4430)$, $Z_b(10610)$, and $Z_b(10650)$ [1]. It would be interesting to see how the four-quark state or the components of a hadron change as the quark masses are changed.

We report the possible significance of the four-quark state in the $I=0$ scalar mesons using two-flavor full lattice QCD simulations[3]. Several quenched lattice simulations for $I=0$ scalar mesons have been carried out [4, 5, 6, 7, 8]. The first full QCD calculations of the σ meson have been investigated by the SCALAR Collaboration[9], where the $\bar{q}q$ interpolating operator only, the obtain $m_\sigma \sim m_\rho$. It was found that the connected and the disconnected diagrams contribute to the σ meson propagator in the same order. Recently, Prelovsek et al. [10] investigated the possibility that the σ meson is well described as a four-quark state, i.e., a molecular or tetraquark state. They omitted the disconnected diagrams. We show that the quark loops given by the disconnected diagrams observed play an essential role in making the four-quark exist. We perform simulations both with and without disconnected diagrams and compare them.

2. Formulation

We adopt the following two types of the operator for four-quark states. The molecular interpolation operator are given by

$$\mathcal{O}^{\text{molec}}(t) = \frac{1}{\sqrt{3}} \left[\mathcal{O}^{\pi^+}(t) \mathcal{O}^{\pi^-}(t) - \mathcal{O}^{\pi^0}(t) \mathcal{O}^{\pi^0}(t) + \mathcal{O}^{\pi^-}(t) \mathcal{O}^{\pi^+}(t) \right], \quad (2.1)$$

where $\mathcal{O}^{\pi^+}(t)$, $\mathcal{O}^{\pi^-}(t)$, and $\mathcal{O}^{\pi^0}(t)$ are the π meson operators made up of two quarks. They are given by

$$\begin{aligned} \mathcal{O}^{\pi^+}(t) &= - \sum_{\mathbf{x}a} \bar{d}^a(t, \mathbf{x}) \gamma_5 u^a(t, \mathbf{x}), \quad \mathcal{O}^{\pi^-}(t) = \sum_{\mathbf{x}a} \bar{u}^a(t, \mathbf{x}) \gamma_5 d^a(t, \mathbf{x}), \\ \mathcal{O}^{\pi^0}(t) &= \frac{1}{\sqrt{2}} \sum_{\mathbf{x}a} [\bar{u}^a(t, \mathbf{x}) \gamma_5 u^a(t, \mathbf{x}) - \bar{d}^a(t, \mathbf{x}) \gamma_5 d^a(t, \mathbf{x})], \end{aligned} \quad (2.2)$$

where a is the index of the color.

The tetraquark interpolation operators are given by

$$\mathcal{O}^{\text{tetra}}(t) = \sum_a [ud]^a(t) [\bar{u}\bar{d}]^a(t), \quad (2.3)$$

where $[ud]^a(t)$ and $[\bar{u}\bar{d}]^a(t)$ are diquark and antidiquark operators, respectively, written as

$$\begin{aligned} [ud]^a(t) &= \frac{1}{2} \sum_{\mathbf{x}b,c} \varepsilon^{abc} \left[u^{Tb}(t, \mathbf{x}) C\gamma_5 d^c(t, \mathbf{x}) - d^{Tb}(t, \mathbf{x}) C\gamma_5 u^c(t, \mathbf{x}) \right], \\ [\bar{u}\bar{d}]^a(t) &= \frac{1}{2} \sum_{\mathbf{x}b,c} \varepsilon^{abc} \left[\bar{u}^b(t, \mathbf{x}) C\gamma_5 \bar{d}^{Tc}(t, \mathbf{x}) - \bar{d}^b(t, \mathbf{x}) C\gamma_5 \bar{u}^{Tc}(t, \mathbf{x}) \right], \end{aligned} \quad (2.4)$$

with the charge conjugation matrix C .

For the interpolation operators of the molecule and tetraquark there are other possible candidates. For example, in Ref. [10], vector- and axial-vector-type operators as well as pseudoscalar-type operators were used for the molecule. For the tetraquark, in addition to the (anti)pseudoscalar diquark operators, the (anti)scalar diquark operators are also employed. The choice of the operators for the molecule and tetraquark is motivated by the fact that pseudoscalar mesons are the lightest mesons and diquarks with $C\gamma_5$ are the lightest diquarks [11].

The propagator $G^i(t)$ for the four-quark operators is written as

$$G^i(t) = \langle \mathcal{O}^i(t) \mathcal{O}^{i\dagger}(0) \rangle, \quad i = \text{molec or tetra}, \quad (2.5)$$

where \mathcal{O}^i is the molecular or tetraquark interpolation operator.

We show the diagrams for the elements of the propagator $G^i(t)$: the molecule $G^{\text{molec}}(t)$ and the tetraquark $G^{\text{tetra}}(t)$. Through the functional integral of Eq. (2.5) with the quark fields, the propagator of the molecular operator $G^{\text{molec}}(t)$ is written as

$$G^{\text{molec}}(t) = 2 \left[D(t) + \frac{1}{2} C(t) - 3A(t) + \frac{3}{2} V(t) \right], \quad (2.6)$$

where $D(t)$, $C(t)$, $A(t)$, and $V(t)$ correspond to direct, crossed, single annihilation (singly disconnected), and vacuum (doubly disconnected) diagrams, respectively (Fig. 1).

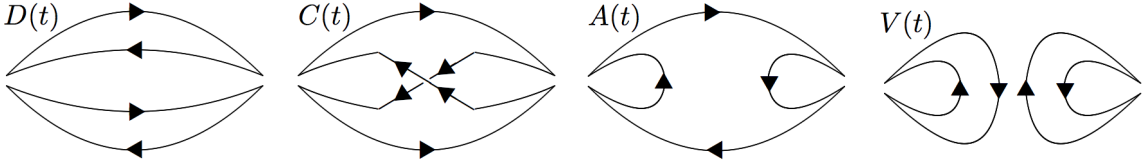


Figure 1: The diagrams for the propagator of the molecular operator $G^{\text{molec}}(t)$.

nected), and vacuum (doubly disconnected) diagrams, respectively (Fig. 1). The detailed expression for each diagram is given in the Appendix. The tetraquark propagator is given by

$$\begin{aligned} G^{\text{tetra}}(t) &= 2 (D'_1(t) + D'_2(t)) - 2 (A'_1(t) + A'_2(t) + A'_3(t) + A'_4(t)) \\ &\quad + (V'_1(t) + V'_2(t) + V'_3(t) + V'_4(t)), \end{aligned} \quad (2.7)$$

where $D'(t)$, $A'(t)$, and $V'(t)$ are shown in Fig. 2. The number index of $D'(t)$, $A'(t)$, and $V'(t)$

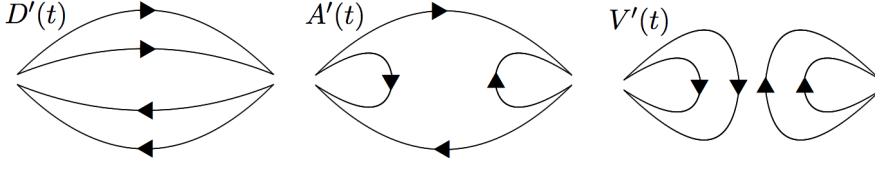


Figure 2: The diagrams for the propagator of the tetraquark operator $G^{\text{tetra}}(t)$.

represents the difference of the combination of the color index. The difference between Figs. 1 and 2 is in the directions of the arrows on the quark lines.

Both propagators $G^{\text{molec}}(t)$ and $G^{\text{tetra}}(t)$ contain doubly disconnected diagrams $V(t)$ and $V'(t)$, which are neglected in our calculations. Assuming that the N_c counting scheme[12] also works for $N_c = 3$, we apply it to the contraction in the diagrams. We estimate the orders of the diagrams in Figs. 1-2: $D(t)$ and $D'(t) \sim \mathcal{O}(N_c^2)$, $C(t) \sim \mathcal{O}(N_c)$, $A(t)$ and $A'(t) \sim \mathcal{O}(N_c)$ and $V(t)$ and $V'(t) \sim \mathcal{O}(1)$. Under the above assumption, we may neglect the doubly disconnected diagrams $V(t)$ and $V'(t)$ compared with other diagrams. Moreover, the large- N_c counting suggests that the singly disconnected diagrams $A(t)$ and $A'(t)$ become the same order as the crossed diagram $C(t)$. The singly disconnected diagrams may play an essential role in the understanding of four-quark states and should not be neglected.

3. Numerical Simulations

We calculate the molecule and the tetraquark propagator in the two-flavor full QCD simulations. We generate the gauge configurations using the same simulation parameters (clover coefficient $C_{SW} = 1.68$ and coupling $\beta = 1.7$) as those in Ref. [13], except for the lattice size. The lattice size in our calculation is set to $8^3 \times 16$, which is smaller than that in Ref. [13]. First we produce the two-flavor full QCD configurations using the hybrid Monte Carlo method with the clover-improved Wilson quark action. The first 2000 trajectories are updated in the quenched QCD, then we switch to simulations with the dynamical fermion. The next 100 hybrid Monte Carlo trajectories are discarded for thermalization; then we start to store the configurations every ten trajectories. The numbers of configurations at the dynamical hopping parameter values of $\kappa = 0.146$, 0.147, and 0.148 are 16496, 14344, and 11720, respectively. Our estimated critical hopping parameter κ_c and the lattice size are $\kappa_c = 0.152(6)$ and $a = 0.269(9)$ fm, respectively. The critical hopping parameter is estimated by the linear extrapolation of the square of the pion mass $(m_\pi a)^2$ as a function of

Table 1: Masses of π and ρ and number of configurations.

| κ | $m_\pi a$ | m_π MeV | $m_\rho a$ | m_ρ MeV | Configurations |
|----------|-----------|-------------|------------|--------------|----------------|
| 0.146 | 1.018(2) | 747(27) | 1.431(4) | 1050(39) | 16496 |
| 0.147 | 0.930(2) | 682(25) | 1.358(6) | 996(38) | 14344 |
| 0.148 | 0.827(4) | 607(23) | 1.304(10) | 956(39) | 11720 |

the inverse of the hopping parameter in Fig. 4. In Fig. 4 we plot rho meson masses as a function of the inverse of the hopping parameter and compute the value of the rho meson mass at the inverse of the critical hopping parameter from the linear extrapolation of the plots. From comparison between the rho meson mass at $1/\kappa_c$, $m_\rho a$ and the physical mass $m_\rho = 770$ MeV, we obtain the lattice spacing $a = 0.269(9)$ fm. We list the values of the π and ρ meson masses together with the number of configurations at $\kappa = 0.146, 0.147$, and 0.148 in Table 1. We calculate the quark propagators using a point source and sink with the clover-improved Wilson quark action. For the disconnected diagrams we employ the Z_2 -noise method with the truncated eigenmode approach. We carry out the dilution in the temporal direction[14], in which the numbers of noise vectors and eigenvalues are 120 and 12, respectively.

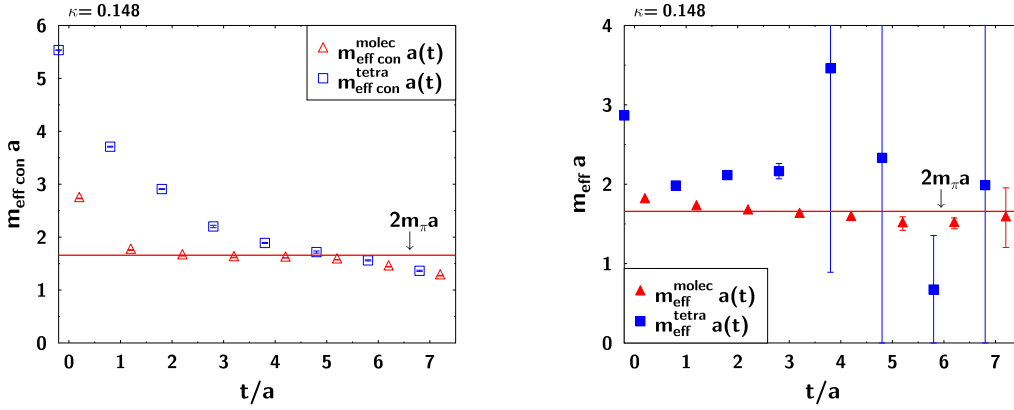


Figure 3: The effective masses of the molecule (open triangles) and tetraquark (open squares) without the singly disconnected diagrams at $\kappa = 0.148$, and the effective masses of the molecule (solid triangles) and tetraquark (solid squares) with the singly disconnected diagrams at $\kappa = 0.148$. The data are plotted at $t/a \pm 0.2$ for visibility.

We show the effective masses obtained from the propagators G^{molec} and G^{tetra} in Fig. 3. The effective masses are defined by

$$\frac{G^i(t)}{G^i(t+1)} = \frac{e^{-m_{\text{eff}}^i(t)t} + e^{-m_{\text{eff}}^i(t)(T-t)}}{e^{-m_{\text{eff}}^i(t)(t+1)} + e^{-m_{\text{eff}}^i(t)(T-(t+1))}}, \quad i = \text{molec or tetra}. \quad (3.1)$$

Figure 3 shows the effective masses without the singly disconnected diagrams as a function of time. The molecule has a clear plateau in the behavior of the effective masses in the range $1 \leq t \leq 5$. The value of the plateau is the same as $2m_\pi$, which would suggest that the molecule has a large overlap with the two-particle π - π scattering state. On the other hand, the values of effective masses of the tetraquark are larger than those of the molecule at small t and decrease significantly with time as reported in Ref.[10]. We do not observe a clear plateau in the effective masses of the tetraquark. At $t = 6, 7$ the small mass drop is found in effective masses of molecule. To understand it we need to check whether the small mass drop still exists in the larger lattice size calculation. Currently we have not reached any physical interpretation of it.

In Fig. 3 we show the effective masses as a function of time for the molecule and tetraquark with the singly disconnected diagrams. The behavior of the effective masses of the molecule with

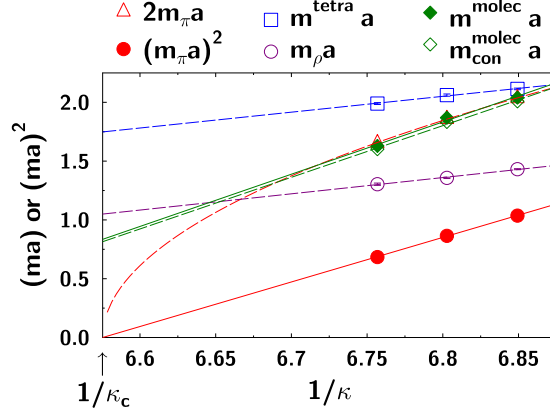


Figure 4: (color online). The quark mass dependence of the square of the π meson mass (solid circles), double the π meson mass (open triangles), the ρ meson mass (open circles), the mass of the molecule (diamonds), and the mass of the tetraquark (open squares). We plot the masses of the molecule both with (solid diamonds) and without (open diamonds) the singly disconnected diagram. The chiral limit is given by $\kappa_c = 0.152(6)$.

the singly disconnected diagram is almost the same as that without the singly disconnected diagram. There is a clear plateau in effective masses whose value is the same as $2m_\pi$. We find a dramatic change in the behavior of the effective masses of tetraquark due to the existence of the singly disconnected diagrams. A plateaulike structure appears at small t whose values are larger than those of molecule, which implies that the tetraquark has a small overlap with the lowest state in the molecule.

In Fig. 4, we display $(m_\pi)^2$, $2m_\pi$, m_ρ , m^{molec} , $m^{\text{molec}}_{\text{con}}$, and m^{tetra} in the lattice unit as a function of the inverse hopping parameter. The masses of the molecular operators are obtained from plateaus of the effective masses in the range $2 \leq t \leq 5$. The difference between the masses of the molecular operator with the singly disconnected diagram and those without the singly disconnected diagram is small at $\kappa = 0.146, 0.147$, and 0.148 . In both cases, the extracted masses are identical to $2m_\pi$ which would suggest that the molecular operators have a large overlap with the two-particle π - π scattering state. To confirm it, the investigation of the energy shift of the two-particle π - π state would be helpful [4, 15]. If we assume that the plateaulike structure of the effective masses of the tetraquark with the singly disconnected diagrams in $1 \leq t \leq 4$ exists, we can evaluate the mass of the tetraquark. The mass from the tetraquark operator is larger than that of the molecular operator and the difference between the masses becomes larger at smaller quark mass. It indicates that the tetraquark operators have smaller overlap with the lowest state in the molecular operators and the mass of them can be a mixture of the excited state. In the calculation, we do not observe any bound four-quark states in the molecular and tetraquark operators.

4. Summary

We explored the possible significance of the four-quark states in $I=0$ scalar channel in lattice

QCD with the two-flavor dynamical quarks. We carried out the results of the effective masses of two types of interpolation operators for the creation of four-quark states, including the estimate of the singly disconnected diagrams, for the first time. We showed that the quark loops given by the disconnected diagrams play an essential role in propagators of molecular and tetraquark operators.

Acknowledgments

The simulation was performed on an NEC SX-9 and SX-ACE supercomputers at RCNP, Osaka University, and was conducted using the Fujitsu PRIMEHPC FX10 System (Oakleaf-FX, Oakbridge-FX) in the Information Technology Center, The University of Tokyo.

References

- [1] K. A. Olive *et al.* [Particle Data Group Collaboration], *Chin. Phys. C* **38**, 090001 (2014).
- [2] R. L. Jaffe, *Phys. Rev. D* **15**, 267 (1977); R. L. Jaffe, *Phys. Rev. D* **15**, 281 (1977).
- [3] M. Wakayama, T. Kunihiro, S. Muroya, A. Nakamura, C. Nonaka, M. Sekiguchi and H. Wada, *Phys. Rev. D* **91**, 094508 (2015) [arXiv:1412.3909 [hep-lat]].
- [4] M. G. Alford and R. L. Jaffe, *Nucl. Phys. B* **578**, 367-382 (2000) [hep-lat/0001023].
- [5] H. Suganuma, K. Tsumura, N. Ishii and F. Okiharu, *Prog. Theor. Phys. Suppl.* **168**, 168 (2007) [arXiv:0707.3309 [hep-lat]].
- [6] N. Mathur, A. Alexandru, Y. Chen, S. J. Dong, T. Draper, I. Horvath, F. X. Lee, K. F. Liu, S. Tamhankar, and J. B. Zhang, *Phys. Rev. D* **76**, 114505 (2007) [hep-ph/0607110].
- [7] M. Loan, Z. H. Luo and Y. Y. Lam, *Eur. Phys. J. C* **57**, 579 (2008) [arXiv:0907.3609 [hep-lat]].
- [8] S. Prelovsek and D. Mohler, *Phys. Rev. D* **79**, 014503 (2009).
- [9] T. Kunihiro, S. Muroya, A. Nakamura, C. Nonaka, M. Sekiguchi, and H. Wada [SCALAR Collaboration], *Phys. Rev. D* **70**, 034504 (2004) [hep-ph/0310312].
- [10] S. Prelovsek, T. Draper, C. B. Lang, M. Limmer, K.-F. Liu, N. Mathur, and D. Mohler, *Phys. Rev. D* **82**, 094507 (2010).
- [11] R. L. Jaffe, *Phys. Rept.* **409**, 1 (2005) [hep-ph/0409065].
- [12] Feng-K. Guo, L. Liu, Ulf-G. Meißner and P. Wang, *Phys. Rev. D* **88**, 074506 (2013).
- [13] A. Ali Khan *et al.* [CP-PACS Collaboration], *Phys. Rev. D* **63**, 034502 (2000) [hep-lat/0008011].
- [14] J. Foley, K. J. Juge, A. Ó. Cais, M. Peardon, S. M. Ryan, and J.-I. Skullerud [TrinLat Collaboration], *Comp. Phys. Comm.* **172**, 145 (2005).
- [15] M. Lüscher, *Commun. Math. Phys.* **104**, 177 (1986); *Commun. Math. Phys.* **105**, 153 (1986); *Nucl. Phys. B* **354**, 531 (1991).